ChemEngineering

MDPI

Article

Environmental Dispersion of Toxic Effluents from Waste Polyethylene Fires: Simulations with ALOFT

Giulia De Cet [1] and Chiara Vianello [1,2,*]

[1] Department of Civil, Environmental and Architectural Engineering, University of Padua, 35131 Padua, Italy; giulia.decet@unipd.it
[2] Department of Industrial Engineering, University of Padua, 35131 Padua, Italy
* Correspondence: chiara.vianello@unipd.it

Abstract: In recent years, the Italian peninsula has frequently been affected by fires in waste storage facilities, both accidental and malicious. Waste storage activities must comply with a series of regulations that require the employer to carefully assess the risks associated with the operation of the plant. All prevention and protection measures must be taken to reduce the risk of fires in order to safeguard both people and the environment. In addition, with new regulations coming into force in November 2022, efforts are being made to regulate waste treatment and storage facilities in terms of fire safety. This work presents simulations of the dispersion into the environment of toxic effluents produced during a polyethylene fire at a storage site, with the aid of dedicated software. Simulations were carried out using ALOFT, varying the parameters of the simulations (e.g., the burnt area, environmental characteristics, and toxic effluent investigated). In total, 24 simulations were carried out to investigate the emissions of particulate matter and volatile organic compounds in the case of polyethylene fires. The simulations showed that atmospheric stability class and wind speed had a significant impact on the dispersion. The proposed methodology can be applied both in the risk assessment and emergency phases and, eventually, as a valuable tool in post-accident analysis.

Keywords: fire; waste materials; simulation; ALOFT; toxic effluent; polyethylene

check for updates

Academic Editor: Airio Egidio Rodrigues

Received: 28 March 2024
Revised: 5 April 2025
Accepted: 10 April 2025
Published: 17 April 2025

Citation: De Cet, G.; Vianello, C. Environmental Dispersion of Toxic Effluents from Waste Polyethylene Fires: Simulations with ALOFT. *ChemEngineering* **2025**, *9*, 41. https://doi.org/10.3390/chemengineering9020041

Copyright: © 2025 by the authors. Licensee MDPI, Basel, Switzerland. This article is an open access article distributed under the terms and conditions of the Creative Commons Attribution (CC BY) license (https://creativecommons.org/licenses/by/4.0/).

1. Introduction

In line with strategic goals of the 2030 UN Agenda related to the Sustainable Development Goals, recent efforts have been made to improve issues related to waste management [1]. Among these goals, there is the decidedly topical issue of waste under No. 12 [2]. Waste management is a critical global challenge that requires innovative solutions and international cooperation [3–5].

In 2020, there were more than two billion tons of waste produced in Europe [6]. This waste material has to be stored before it is recycled or incinerated, and this waste storage may incur dangers related to fires, which can have severe environmental consequences. The potential for fires in waste storage facilities poses significant risks to both human health and the environment, necessitating improved safety measures and monitoring systems [7–9]. Case studies of fires in waste storage facilities in Norway and Sweden highlight the issues related to collecting reliable data from these types of fires, providing useful information with respect to carrying out fire safety assessments in order to increase the level of safety in these facilities [8].

In Italy, there has been an increase in waste storage facility fires in recent years. Between 2014 and 2017, there were more than 250 events distributed as follows: 52.6% in

the north, 13.8% in the center and 21.6% in the south. There were more fires in the north because there are more waste management facilities located there, in conjunction with greater urbanization and industrialization [10]. The geographical distribution of these fires highlights the need for targeted interventions and region-specific strategies to address the issue effectively.

The ignition sources of these fires varied and, as such, a governing body called "the Parliamentary committee of Inquiry for illicit facts connected with the waste cycle and the related environmental illicit facts" (i.e., Commissione parlamentare d'inchiesta sulle attività illecite connesse al ciclo dei rifiuti e agli illeciti ambientali collegati), formed in 2014, approved a relation on 28 March 2018, in which several kinds of events were taken into account. The establishment of specialized committees to investigate waste-related crimes demonstrates the growing recognition of the complex nature of this problem and the need for a multidisciplinary approach. It has not been determined why there has been an increase in the number of these fires in Italy; the reasons could be related to insufficient control and surveillance systems (to prevent arson), a failure of controls, or an overload of material. As such, these types of fires are difficult to study due to their unknown causes/origins, but they are important with respect to understanding the risks posed to people living nearby. In the past, the focus has been on the consequences that these fires may have for air, water, and soil, but now the focus is also on three other dimensions—ecological, economic, and social [11]. The shift towards a more holistic approach in assessing the impact of waste fires reflects a growing awareness of the interconnectedness of environmental, economic, and social factors in sustainability.

In another case study of a waste disposal plant [12], the fire was found to have originated from a collection of unsorted municipal waste, which then spread to other materials. The authors modeled this fire using the Fire Dynamics Simulator (FDS) and outlined numerous future potential developments; this opened up an important discussion about the effectiveness of using these models for fire investigation. Although the ignition sequence was calibrated to the observed data, the simulation carried out by the authors was not able to correctly address the propagation of the fire to the surrounding poles. This result can probably be attributed to the uncertainty and limitations in the definition of the combustible matrices (the actual properties were not known). The use of advanced modeling techniques such as FDS represents a significant step forward in understanding and predicting fire behavior in complex waste storage environments.

Romano and Romano reconstructed the evolution of a fire that occurred in northern Italy in 2017, using FDS and PyroSim [13]. The authors made a three-dimensional simulation of the fire. They assumed that the fire started from a waste accumulation. Considering the presence of concrete walls and the ignition temperature, the simulation yielded results that were compatible in terms of the timing of the fire's development. These simulation techniques offer valuable insights into fire dynamics and can potentially inform the design of more effective fire prevention and containment strategies in waste management facilities.

Outside of waste management facilities, unfortunately, there has been an increase in the amount of toxic and special waste being burned and buried in southern Italy, resulting in many unauthorized dumps that are typically set on fire to reduce the waste. The proliferation of illegal waste disposal practices poses a significant challenge to environmental protection efforts and requires a coordinated response from law enforcement and environmental agencies.

The environmental impact of this is not well understood; as such, it has been determined that there is a need to combat the use of illicit fires in these areas. These fires have increased the damage to buildings and the surrounding environment caused by the uncontrolled incineration and trafficking of waste [14]. This team proposed a mathematical

model that can generate a municipal environmental pressure index. The model is useful for an assessment, on a municipal (or aggregation of municipalities) basis, of environmental pressure. It is also designed for the planning and monitoring of improvement actions on a larger (local or regional) scale. In some areas of southern Italy in particular, not many areas have been reclaimed, and these models could help to identify areas to be reclaimed. Moreover, biomonitoring is increasingly a pressing need.

Moreover, Falcone and De Rosa [15] proposed an analytical method to apply to these illicit burning sites aims to develop policy strategies capable of optimizing municipal waste management systems (MWMSs) through the use of fuzzy cognitive maps (FCMs). Using causal reasoning, the FCM method determines the behavioral complexity of a system through a participatory modelling approach [16]. Their work identified how information campaigns and technological innovation could improve MWMSs. The application of advanced analytical methods such as FCMs demonstrates the potential for innovative approaches in addressing complex waste management challenges.

Mazza et al. [17] reviewed 18 epidemiological studies, analyzing both environmental and population health consequences. The authors concluded that Naples and the Campania region could be a perfect context for developing models to examine human and environmental contamination. The focus on epidemiological studies in regions heavily affected by waste mismanagement highlights the critical link between environmental degradation and public health, emphasizing the urgency of addressing these issues [18–20].

In this study, after offering an overview of fire prevention regulations, the authors identified plastic as the material that simulates different kinds of fires. This choice was dictated by the fact that, in Italy, plastic in waste represents a significant percentage (≈10%) of the total, and it has a greater impact on the environment in the event of fires [21]. For this reason, the authors considered it reasonable to investigate polyethylene—which accounts for 40% of the total volume of plastics production worldwide—in this first study. The focus on plastic waste in fire simulations reflects the growing concern over the environmental impact of plastic pollution and the need for improved recycling and disposal methods. The aim of our study is, therefore, to employ software for modelling the polyethylene fire plume. Moreover, numerical modelling is a valuable tool that can be fruitful in different analytical phases. First and foremost, it can be beneficial in the risk assessment and estimation phase, but also in the operational-accident phase, to estimate the consequences in real-time, and finally, as a tool for the post-accident evaluation. The novelty of this work lies in its comprehensive approach to addressing the environmental dispersion of toxic effluents from waste polyethylene fires through numerical simulations. The authors employed ALOFT version 3.10 (NIST SP 924), a dedicated software tool developed by the National Institute of Standards and Technology, to model and analyze the dispersion patterns of key pollutants, such as particulate matter and volatile organic compounds, under various fire scenarios.

One of the notable contributions of this study is the systematic investigation of the impact of different parameters on the dispersion of toxic effluents. The authors have conducted a series of simulations, varying factors such as the fire surface area, wind speed, atmospheric stability class, and downwind distance. This comprehensive approach provides valuable insights into the interplay between these variables and their influence on the dispersion patterns, enabling a more informed assessment of potential environmental impacts. The development of sophisticated modeling tools for fire plume analysis represents a significant advancement in our ability to predict and mitigate the environmental impacts of waste fires.

The work is intended to be a starting point for developing and validating a methodology that can be employed, as illustrated above, in several possible preventive and operational phases. However, the model predictions were compared, in a previous study [22],

with measurements taken during three field experiments. This comparative approach between model predictions and field experiments is crucial for validating and refining our understanding of fire behavior in waste management contexts.

2. Background

2.1. Evolution of Fire Prevention Regulations

Overall, fire prevention today is rooted in a complex system of rules, standards, and circulars. An abundant body of legislation supports the fire prevention planner. The evolution of fire prevention legislation in Italy dates back to 1955, when Articles 36 and 37 of Presidential Decree no. 547 of 27 April 1955 established that, before undertaking an activity involving employees, it was necessary to request approval of the project for fire safety. The approval had to come from the relevant Provincial Fire Brigade Command. Subsequently, through the natural development of legislation, we arrived at Presidential Decree no. 151 of 2011, which introduces the Certified Activity Start Notice (i.e., Segnalazione Certificata di Inizio Attività, SCIA) as its main novelty. Presidential Decree no. 151 [23] radically transformed the technical–administrative procedures, simplifying them to speed up the process. Presidential Decree no. 151 is the regulation that identifies the activities subject to fire prevention controls. Annex I lists and classifies all the activities subject to fire prevention controls divided into categories A, B, and C in relation to the sector and size of the activity, the need to protect public safety and the existence of technical rules. Category A includes activities that relate to 'technical regulation' and are characterized by a limited level of complexity linked to the size of the activity, crowding, and the quantity of material. Category B includes activities present in A, in terms of type, yet they are characterized by a greater level of complexity, as well as activities that do not have a specific related technical regulation, but, in any case, exhibit a level of complexity lower than the parameter assumed for the 'higher' category. Finally, Category C contains all those activities with a high level of complexity, regardless of the presence or absence of a 'technical regulation'.

In addition to the identification of activities and their classification, this decree governs and regulates the examination of projects, technical visits, the issue of exemptions and all other competencies of firefighters. The subject activities covered by the case study—as far as the storage of solid waste is concerned—are located at numbers 34, 36, 43, 44, 55, and 70.

In addition to identifying and classifying activities, this decree governs and regulates the examination of projects, technical inspections, the issue of exemptions, and all others. The real innovation came with the Ministerial Decree of 3 August 2015, called the 'Fire Prevention Code' [24]. These technical standards can be applied to both existing and new activities. The code presents the methodologies for fire safety design to be implemented in order to achieve the primary objectives of fire prevention. The code is based on eight principles that make it revolutionary compared to many of the pre-existing regulations:

1. Generality: the code outlines the fire safety design methodologies that can be applied to all activities;
2. Simplicity: it emphasizes that easier, more feasible and understandable solutions are preferred, as they are also easier to maintain;
3. Modularity: the complexity of the subject is divided into easy modules, which are aimed at guiding the designer to the appropriate design for any specific activity;
4. Flexibility: each fire safety performance for an activity corresponds to multiple prescriptive or performance design solutions. The recognized methods are defined here, so that the designer can independently conceive and demonstrate the validity of the alternative design solution in compliance with the fire safety objectives;

5. Standardization and integration: it ensures that the language of fire prevention complies with international standards. Provisions from pre-existing Italian documents are also integrated;
6. Inclusion: the different disabilities (e.g., motor, sensory, cognitive), temporary or permanent, of those involved in the activities, are of course considered an integral part of fire safety design;
7. Evidence-based content: the content is based on the research, evaluation, and systematic use of the data, originating from national and international research within fire safety;
8. Updatability: the whole code is created in a way that allows for effortless modifications so that it can evolve with the continuous advancement of technology and knowledge.

The code defines a horizontal technical regulation as a fire prevention regulation applicable to all activities and a vertical technical regulation as one appropriate to a specific activity or areas of it, with specific indications complementary to or in place of those provided for in the horizontal technical regulation. With regard to establishments and waste storage and treatment plants, from November 2022 in Italy, the vertical technical rule comes into force, laying down precise indications and overcoming the numerous guidelines and circulars that, with practical solutions, tried to prevent and manage accidental events. The code has incorporated elements for the simplification and rationalization of the regulatory corpus. Strength and innovation are approaching the code certainly offers, with the intention of achieving high safety standards while sewing together flexible techniques and appropriate solutions that are outlined ad hoc for each case.

2.2. The Combustion of Plastics

Combustion can be classified into three categories: homogeneous (e.g., combustion of gaseous substances), heterogeneous (e.g., combustion of solid and liquid substances) and condensed systems (e.g., explosives). In the case of plastics, combustion is heterogeneous.

Plastics subjected to fire can be evaluated according to different regulations, using test methods and according to the presence or absence of retardant agents, such as halogenates or phosphorous, which are capable of retarding the spread of flames.

Toxic gases and fumes, which are harmful to both human health and the environment, are released during combustion [25–27].

Such emissions can create a high level of opacity that hinders the proper escape route; as far as open spaces are concerned, fumes can instead have an impact on the population, on neighboring activities, and on the environment. Therefore, the parameters that are assessed in an analysis when burning these materials are the density of the fumes released and their toxicity. When assessing the risk, it is thus essential to consider the presence or absence of flame-retarding halides.

The simulations presented in this article focused on polyethylene (PE). It is the most widespread polymer and is used for manufacturing plastic bags, bottles, jerrycans and caps, bottles for foodstuffs, detergents and chemical agents, boxes, and films of various thicknesses for agricultural, industrial, and construction use. Polyethylene is the most common and cost-effective plastic; it is used everywhere and can be processed easily. These are some of the reasons why this material was chosen for the following simulation [28–32]. In addition, PE is a recyclable plastic material and, in 2022, Italy was is among the top three nations for plastic recycling capacity, particularly polyethylene [33]. Its high calorific value is about 40 MJ/kg [34]. As mentioned previously, during combustion, several gases can be produced, and the type of material being burned dictates the nature of these gases. In the case of PE, these include cyclic and aromatic hydrocarbons, PAH, VOC, CO, and CO_2 [26,35].

3. Methodology

ALOFT-FT® (A Large Outdoor Fire Plume Trajectory model—Flat Terrain) is a software produced by the NIST. This approach draws inspiration from the one proposed by Ghoniem and colleagues [36], but it distinguishes itself by employing finite-difference methods to analyze large-scale mixing. Additionally, it incorporates a Lagrangian description to track the movement of smoke and other pollutants. It is relevant to this topic as it models the downwind distribution of combustion products and the concentration of smoke from large outdoor fires [22,37,38]. The modelling of the fire scenario was performed using the ALOFT programme version 3.10 (NIST SP 924). There is a public-domain version for Windows; in this case, the simulations were conducted using a Windows XP Home Edition 2002 virtual machine.

3.1. Plume Dynamics

The release of smoke from a fire can be modelled as a plume of smoke [39–42]. As far as the downwind length of the plume is concerned, the shape and extension of the plume depends on wind speed and atmospheric stability [36,43]. Pasquill Giffort's classes are indicators of atmospheric turbulence; there are six classes, with further subdivisions, according to various atmospheric conditions as stability changes (A: Extremely unstable; B: Moderately unstable, C: Slightly unstable, D: Neutral, E: Slightly stable, F: Moderately stable) [44]. The stability category corresponds to the standard deviation values of the prevailing wind direction in the horizontal and vertical directions. There is an extensive discussion of these parameters and the methods of assessing them in the literature [45]. Usually, the smoke plume resides mainly in what is called the planetary boundary layer. Sometimes this region is also called the mixing layer, although the precise definition of these terms varies depending on the specific application [22].

The plume behavior is also influenced by the phenomenon of thermal inversion. As the sea level rises, there is a progressive increase in temperature; the adiabatic temperature gradient takes on values less than zero. For altitudes below 200 m, the dispersion of pollutants is strongly inhibited by stable conditions.

The movements of the effluent are influenced by temperature and height. The associated phenomena are analogous to the effect of the buoyancy forces expressed by Grashof [46].

Experiments revealed that simple smoke models do not capture the characteristics of the oblique plume and the downwind distribution is not Gaussian [37]. To solve this problem, the National Institute of Standard and Technology (NIST) developed a smoke plume trajectory model, discussed below.

3.2. Plume Trajectory Model

Every iteration of the ALOFT model incorporates discretized motion equations that describe how heat, smoke particles, and other combustion byproducts enter the atmosphere. These fire-related variables are determined through both laboratory and field studies. This section explores how these equations are simplified to make them solvable using current computer workstations and, in some instances, personal computers. The ALOFT-FT model employs a simplified approach based on a unidirectional wind field to estimate plume rise and downwind transport over flat landscapes. When a substantial blaze releases smoke and heated gases into the surrounding air, this process can be characterized using fundamental physical principles. Specifically, the laws of conservation—applied to mass (Equation (1)), momentum (Equation (2)), and energy (Equation (3))—provide a framework

for understanding how these emissions affect key atmospheric properties. These properties include the air's temperature, pressure, density, and movement patterns:

$$\text{Conservation of mass}: \ \frac{\partial \rho}{\partial t} + \nabla \times \rho \mathbf{u} = 0 \tag{1}$$

$$\text{Conservation of momentum}: \ \rho\left(\frac{\partial \mathbf{u}}{\partial t} + (\mathbf{u} \times \nabla)\mathbf{u}\right) + \nabla p - \rho g = \nabla \times \sigma \tag{2}$$

$$\text{Conservation of energy}: \ \rho c_p\left(\frac{\partial T}{\partial t} + \mathbf{u} \times \nabla T\right) - \frac{dp}{dz} = \dot{q} + \nabla \times k\nabla T \tag{3}$$

$$\text{Equation of state}: \ p = \rho R T \tag{4}$$

where:

- ρ is density;
- $\mathbf{u}$ is the velocity vector (u, v, w);
- p is pressure;
- g is the gravity vector;
- c_p is the constant-pressure specific heat;
- T is the absolute temperature;
- k is the thermal conductivity;
- t is the time;
- $\dot{q}$ is the prescribed volumetric heat release rate;
- R is the gas constant equal to the difference of the specific heats ($R = c_p - c_v$);
- σ is the standard stress tensor for compressible fluids.

To facilitate numerical computations, these equations need to be simplified. The ALOFT-FT model employs the Boussinesq approximation, a method that treats the fluid as largely incompressible while accounting for buoyancy-driven flow. This flow arises from the temperature difference between the heated smoke plume gases and the ambient atmosphere. Panotsky and Dutton provide a thorough validation of this approximation, which is briefly outlined here. The initial assumption is that pressure can be decomposed into two components: a hydrostatic term and a perturbation term influenced by fire and terrain factors (as shown in Equation (5)). The Cartesian coordinate system is defined by the vector $\mathbf{x}$ = (x, y, z), where z represents the vertical axis. Temperature and density fields undergo a similar decomposition process (refer to Equations (6) and (7) for details). The relationship between ambient pressure and density is governed by the hydrostatic condition, as illustrated in Equation (8). It is important to note that the variations in ambient parameters T_0, p_0 and ρ_0 are considered minimal compared to their sea-level values. A key implication of the Boussinesq approximation is the simplification of the convective derivative. Specifically, the term $\frac{dp}{dt} = \frac{\partial p}{\partial t} + \mathbf{u} \times \nabla p$ in Equation (3) is approximated as $w\frac{dp_0}{dz}$. This modification effectively removes acoustic waves from the solution, significantly streamlining the numerical computation process. As a result, the time step in the calculations is no longer constrained by sound speed limitations.

The Boussinesq formulation of the governing equations is presented in Equations (9) through (12), reflecting these simplifications and assumptions.

It is worth highlighting that the dissipation components have been streamlined under the assumption of constant viscosity (μ) and thermal conductivity (k) coefficients.

$$p(x, t) = p_0(z) + \widetilde{p}(\mathbf{x}, t) \tag{5}$$

$$T(\mathbf{x}, t) = T_0(z) + \widetilde{T}(\mathbf{x}, t) \tag{6}$$

$$\rho(\mathbf{x}, t) = \rho_0(z) + \tilde{\rho}(\mathbf{x}, t) \tag{7}$$

$$\frac{dp_0}{dz} = -\rho_0 g \tag{8}$$

$$\text{Conservation of mass (incompressibility)}: \ \nabla \times \mathbf{u} = 0 \tag{9}$$

$$\text{Conservation of momentum}: \ \rho_0\left(\frac{\partial \mathbf{u}}{\partial t} + (\mathbf{u} \times \nabla)\mathbf{u}\right) + \nabla\tilde{p} - \tilde{\rho} g = \mu\nabla^2\mathbf{u} \tag{10}$$

$$\text{Conservation of energy}: \ \rho_0 c_p\left(\frac{\partial \tilde{T}}{\partial t} + \mathbf{u} \times \nabla\tilde{T}\right) - \left(\frac{dp_0}{dz} - \rho_0 c_p \frac{dT_0}{dz}\right)w = \dot{q} + k\nabla^2\tilde{T} \tag{11}$$

$$\text{Equation of state}: \ \frac{\rho - \rho_0}{\rho_0} = \frac{T - T_0}{T_0} \tag{12}$$

The ALOFT-FT model is built on the premise that, within approximately 1 km of a fire, the wind field is largely unidirectional, moving at a minimum speed of 1–2 m/s. It also assumes relatively flat terrain near the fire site. These foundational assumptions enable a technique known as parabolization, which simplifies the governing equations by eliminating time-dependent terms, treating the upwind velocity component as constant, and substituting the upwind spatial coordinate with a temporal one.

Following appropriate non-dimensionalization, the original three-dimensional, steady-state equation system is transformed into a two-dimensional, time-dependent framework.

These simplified equations can resolve plume ascent down to a 5–10 m scale, effectively capturing air entrainment into the smoke column. The high spatial resolution achieved using this simplification method makes these equations suitable for describing plume rise in the ALOFT-FT model.

The parabolization process assumes that the dominant wind maintains a relatively steady speed and direction, aligned with the positive x-axis. Cross-wind velocity components (v, w) are confined to a plane (y, z) perpendicular to the ambient wind direction (x). The uniform ambient wind speed is denoted as U_0.

For fire characterization, only two parameters are required: the overall convective heat release rate (Q) and the particulate mass flux (M). The initial temperature distribution across the plume's cross-section is modeled as Gaussian, conforming to a specific integral equation (see Equation (13)). The particulate distribution is set up in a comparable manner, conforming to the integral presented in Equation (14), where ρ_p denotes the particulate matter's density (units of mass per unit volume). In the software simulations, particulate matter is tracked using Lagrangian particles [12].

The Boussinesq form of the governing equations is scaled based on the fire's intensity. Equation (15) defines the length scale, with the subscript "∞" indicating ground-level ambient conditions, and N_0 representing the Brunt–Väisälä frequency typical of the lower atmosphere. This length scale L approximates the plume's height:

$$\int_{-\infty}^{\infty}\int_{0}^{\infty} \rho_0 c_p U_0 \tilde{T} dz dy = Q \tag{13}$$

$$\int_{-\infty}^{\infty}\int_{0}^{\infty} \rho_p U_0 dz dy = M \tag{14}$$

$$L = \left(\frac{Qg}{c_p T_\infty \rho_\infty U_0 {N_0}^2}\right)^{1/3} \tag{15}$$

$$t^* = \frac{N_0}{U_0}x \tag{16}$$

$$V = N_0 L \tag{17}$$

$$(y, z) = fL(y^*, z^*) \tag{18}$$

$$(v, w) = fL(v^*, w^*) \tag{19}$$

$$\tilde{T} = \frac{fQ}{c_p \rho_\infty U_0 L^2} \tilde{T}^* \tag{20}$$

$$Re = \frac{f^2 \rho_\infty VL}{\mu} \tag{21}$$

$$Pr = \frac{\mu c_p}{k} \tag{22}$$

A temporal coordinate replaces the upwind spatial coordinate x, as shown in Equation (16). The characteristic air velocity in the crosswind plane is given by Equation (17).

Equations (18) and (19) use the characteristic length L and velocity V to define dimensionless crosswind spatial coordinates (y*, z*) and velocities (v*, w*). An adjustable scale factor f ensures the plume height does not exceed the computational domain's height, fL.

Equation (20) defines the non-dimensional temperature perturbation $\tilde{T}^*$. Lastly, Equations (21) and (22) present the turbulent Reynolds and Prandtl numbers, respectively.

The conservation laws are given in Equations (23)–(26) under the condition given in Equations (27) and (28).

$$\text{Conservation of mass (incompressibility)}: \quad \frac{\partial v^*}{\partial y^*} + \frac{\partial w^*}{\partial z^*} = 0 \tag{23}$$

$$\text{Conservation of momentum}: \quad \frac{\partial v^*}{\partial t^*} + v^* \frac{\partial v^*}{\partial y^*} + w^* \frac{\partial v^*}{\partial z^*} + \frac{\partial \tilde{p}^*}{\partial y^*} = \frac{1}{Re}\left(\frac{\partial^2 v^*}{\partial y^{*2}} + \frac{\partial^2 v^*}{\partial z^{*2}}\right) \tag{24}$$

$$\text{Conservation of momentum}: \quad \frac{\partial w^*}{\partial t^*} + v^* \frac{\partial w^*}{\partial y^*} + w^* \frac{\partial w^*}{\partial z^*} + \frac{\partial \tilde{p}^*}{\partial z^*} - \tilde{T}^* = \frac{1}{Re}\left(\frac{\partial^2 w^*}{\partial y^{*2}} + \frac{\partial^2 w^*}{\partial z^{*2}}\right) \tag{25}$$

$$\text{Conservation of energy}: \quad \frac{\partial \tilde{T}^*}{\partial t^*} + v^* \frac{\partial \tilde{T}^*}{\partial y^*} + w^* \frac{\partial \tilde{T}^*}{\partial z^*} + N^{2*} w^* = \frac{1}{RePr}\left(\frac{\partial^2 \tilde{T}^*}{\partial y^{*2}} + \frac{\partial^2 \tilde{T}^*}{\partial z^{*2}}\right) \tag{26}$$

$$v^*(y^*, z^*, t = 0) = w^*(y^*, z^*, t = 0) = 0 \tag{27}$$

$$\int_{-\infty}^{\infty} \int_{0}^{\infty} \tilde{T}^*(y^*, z^*, t = 0) dy^* dz^* = \frac{1}{f^3} \tag{28}$$

At the outset of the model, the cross-flow velocity components, denoted as v and w, are set to zero. However, it is important to note that this initial condition is not a rigid constraint on the system. The model incorporates specific boundary conditions at ground level, namely, the no-flux and free-slip conditions. These boundary specifications are chosen to align with two key assumptions: the presumed uniformity of the prevailing wind and the inherent resolution limitations of the computational process. This approach provides a balanced starting point for the simulation while allowing for realistic development of the flow field as the calculation progresses.

An estimate of the maximum ground level concentration is given by Equation (29). The maximum concentration is reached according to Equation (30) and, if the maximum concentration exceeds the given critical concentration, according to Equation (31).

$$\rho_{max} = \frac{M}{Q^{\frac{2}{3}}}\left(\frac{U_0}{U_{eq}}\right)^{\frac{2}{3}}\left(\frac{\Gamma - \Gamma_{ad}}{T_\infty}\right)^{\frac{2}{3}}(31.6 - 0.480U_{eq})\left(\frac{\mu g}{m^3}\right) \quad (29)$$

$$x_{max} = \sqrt{\frac{T_\infty}{\Gamma - \Gamma_{ad}}}(11.6 - 3.11U_{eq})(m) \quad (30)$$

$$x_c = x_{max} + 23.2\sqrt{\frac{-T_\infty \ln\left(\frac{\rho_c}{\rho_{max}}\right)}{\Gamma - \Gamma_{ad}}}(m) \quad (31)$$

where:

- ρ_{max} is the maximum concentration;
- ρ_c is the critical concentration;
- M is the mass generation rate of any combustion product interest (µg/s);
- Q is the heat release rate (W);
- U_0 is the wind speed (m/s);
- U_{eq} is the equivalent wind speed (m/s);
- Γ is the temperature lapse rate (°C/m);
- Γ_{ad} is the dry adiabatic lapse rate −0.0097 (°C/m);
- T_∞ is the ground temperature (K);
- x_{max} is the distance of maximum concentration downwind of the fire (m);
- x_c is the distance of critical concentration downwind of the fire (m).

It is important to acknowledge that the atmospheric turbulence model presented here is relatively basic. More complex models are available in the literature. Readers interested in further exploration are encouraged to consult various references that offer correlations based on a range of observed conditions [43,45–49]. While an anemometer provides the most accurate wind fluctuation data, it is often difficult to obtain such specific information for a particular area and set of atmospheric conditions.

3.3. Data Input

Using ALOFT, different simulations were carried out to evaluate possible fire scenarios for PE. In total, 24 scenarios were indeed examined. Particulate matter (PM10) emissions were investigated by creating 12 specific simulations and changing the parameters shown in Figure 1 and Table 1. The parameters were taken from the literature [50–54]. The ALOFT software introduces some simplifications compared to the classes established by Pasquill.

The same process was later repeated for volatile organic compounds (VOCs), as reported in the 12 simulations in Table 1. Assuming that the fire took place on the Italian territory, the following variables were related to the environment: the temperature value (25 °C). Moreover, the wind speed and the relative Pasquill class (D and F) were varied. Distances were chosen in a more limited area (1 km) and the surrounding areas (5 km).

De Cet [55] carried out case studies, based on Italian regulations, of waste storage fires in Italy, in which the areas were 4.8 and 48 m^2. However, the ALOFT software does not allow for the simulation of areas smaller than 25 m^2. The authors therefore considered it appropriate not only to simulate 48 m^2 (which we approximated to 50), but also to add two other quantities of stored material to study how and how much the emissions vary as the surface area of the fire changes.

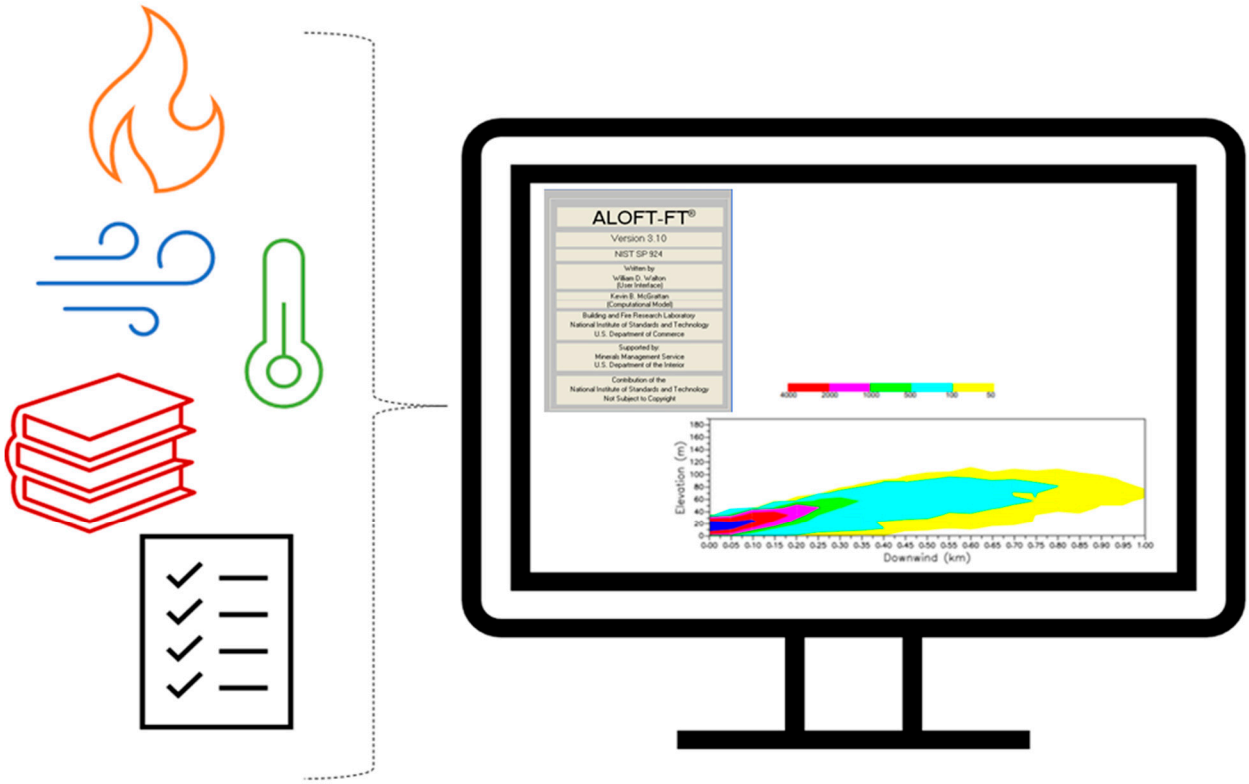


Figure 1. The simulation process using the ALOFT-FT software version 3.10 (NIST SP 924), where various input parameters such as fire characteristics, atmospheric conditions (represented by icons for flames, wind, and temperature) are provided. These inputs are fed into the software to perform the simulation and generate outputs, such as the plume trajectory plot shown on the computer screen. The simulation aims to model the behavior and dispersion of smoke and pollutants from outdoor fires under different scenarios.

Table 1. Simulation parameters. Sim: simulation; DD: downwind distance; HRR: heat release rate per unit area, RF: radiative fraction; BR: burning rate per unit area; WS: wind speed; ET: environmental temperature.

Sim.	DD (km)	Fires' Surface (m^2)	HRR (MW/m^2)	RF (−)	BR (kg/m^2s)	Emission (g/kg)	Effluent	Pasquill Class	WS (m/s)	ET (°C)
1	1	50	0.145	0.381	0.00309	29.63	PM10	D	5	25
2	5	50	0.145	0.381	0.00309	29.63	PM10	D	5	25
3	1	50	0.145	0.381	0.00309	29.63	PM10	F	2	25
4	5	50	0.145	0.381	0.00309	29.63	PM10	F	2	25
5	1	100	0.145	0.381	0.00309	29.63	PM10	D	5	25
6	5	100	0.145	0.381	0.00309	29.63	PM10	D	5	25
7	1	100	0.145	0.381	0.00309	29.63	PM10	F	2	25
8	5	100	0.145	0.381	0.00309	29.63	PM10	F	2	25
9	1	1000	0.145	0.381	0.00309	29.63	PM10	D	5	25
10	5	1000	0.145	0.381	0.00309	29.63	PM10	D	5	25
11	1	1000	0.145	0.381	0.00309	29.63	PM10	F	2	25
12	5	1000	0.145	0.381	0.00309	29.63	PM10	F	2	25
13	1	50	0.145	0.381	0.00309	2.4	VOC	D	5	25
14	5	50	0.145	0.381	0.00309	2.4	VOC	D	5	25

Table 1. *Cont.*

Sim.	DD (km)	Fires' Surface (m^2)	HRR (MW/m^2)	RF (−)	BR (kg/m^2s)	Emission (g/kg)	Effluent	Pasquill Class	WS (m/s)	ET (°C)
15	1	50	0.145	0.381	0.00309	2.4	VOC	F	2	25
16	5	50	0.145	0.381	0.00309	2.4	VOC	F	2	25
17	1	100	0.145	0.381	0.00309	2.4	VOC	D	5	25
18	5	100	0.145	0.381	0.00309	2.4	VOC	D	5	25
19	1	100	0.145	0.381	0.00309	2.4	VOC	F	2	25
20	5	100	0.145	0.381	0.00309	2.4	VOC	F	2	25
21	1	1000	0.145	0.381	0.00309	2.4	VOC	D	5	25
22	5	1000	0.145	0.381	0.00309	2.4	VOC	D	5	25
23	1	1000	0.145	0.381	0.00309	2.4	VOC	F	2	25
24	5	1000	0.145	0.381	0.00309	2.4	VOC	F	2	25

ALOFT has an internal database with certain types of fuels and provides the possibility of including others. When inserting a new fuel type, it is necessary to know the following parameters relating to the heat release rate curve, the radiant fraction, and the fuel consumption per unit of time. It is also possible to enter the fraction of combustion products. In the present simulation, the parameters for PE were taken from the literature [50,56–59]. Table 1 shows the input data of the simulation studies carried out for PM10 and VOC emissions in the case of polyethylene fires. The only difference in the simulations between PM10 and VOC is the emission value entered into the software database.

4. Results and Discussion

As previously described, 24 simulations were carried out to investigate the emissions of PM10 and VOC in the case of polyethylene fires. The results obtained are presented below.

4.1. Emissions of Particulate Matter—PM10

The first four simulations are all characterized by the same fire surface area of 50 m^2. The first two simulations share a wind velocity of 5 m/s. In simulation 1, the height of the initial plume is about 42 m (see Figure 2). It is observed that, as the distance increases, the height of the cloud increases in its turn, until reaching almost 95 m at a distance of 557 m. Initially, there is a concentration of PM10 between 2000 and 4000 $\mu g/m^3$; after the first 300 m it is reduced to 100–500 $\mu g/m^3$. The cloud begins to rise from the ground at a distance of 360 m. At a distance of 557 m downwind, the cloud is at a height of 32 m above the ground, with concentrations of less than 100 $\mu g/m^3$. At this point, the cloud disperses with a concentration of less than 50 $\mu g/m^3$ at a distance of 858 m. It is clear that the modelled plume disperses with a concentration of less than 50 $\mu g/m^3$ before 1 km (Figure 2).

As we move on to the description of simulations 3 and 4, we can observe how these differ from the previous two simulations. This time, the wind speed is 2 m/s. Reducing the wind speed (simulations 1–2 vs. simulations 3–4) shows how the smoke disperses over greater distances. Moving to simulation 3, the height of the initial plume is about 44 m (see Figure 2). It is observed that, as the distance increases, the height of the cloud also increases, until it reaches almost 130 m at a distance of 402 m. Initially, there is a concentration of PM10 of more than 4000 $\mu g/m^3$; after the first 200 m, it is reduced to 100–500 $\mu g/m^3$. The cloud begins to rise from the ground at a distance of 5 m. At a distance of 302 m downwind, the cloud is at a height of 115 m above the ground, with concentrations of

less than 100 μg/m^3. The plume is not dispersed within 1 km. We can then continue the description with simulation 4, which, unlike simulation 3, has a downwind distance of 5 km. After the first km, the plume is at a height of 70 m above the ground with concentrations between 50 and 500 μg/m^3.

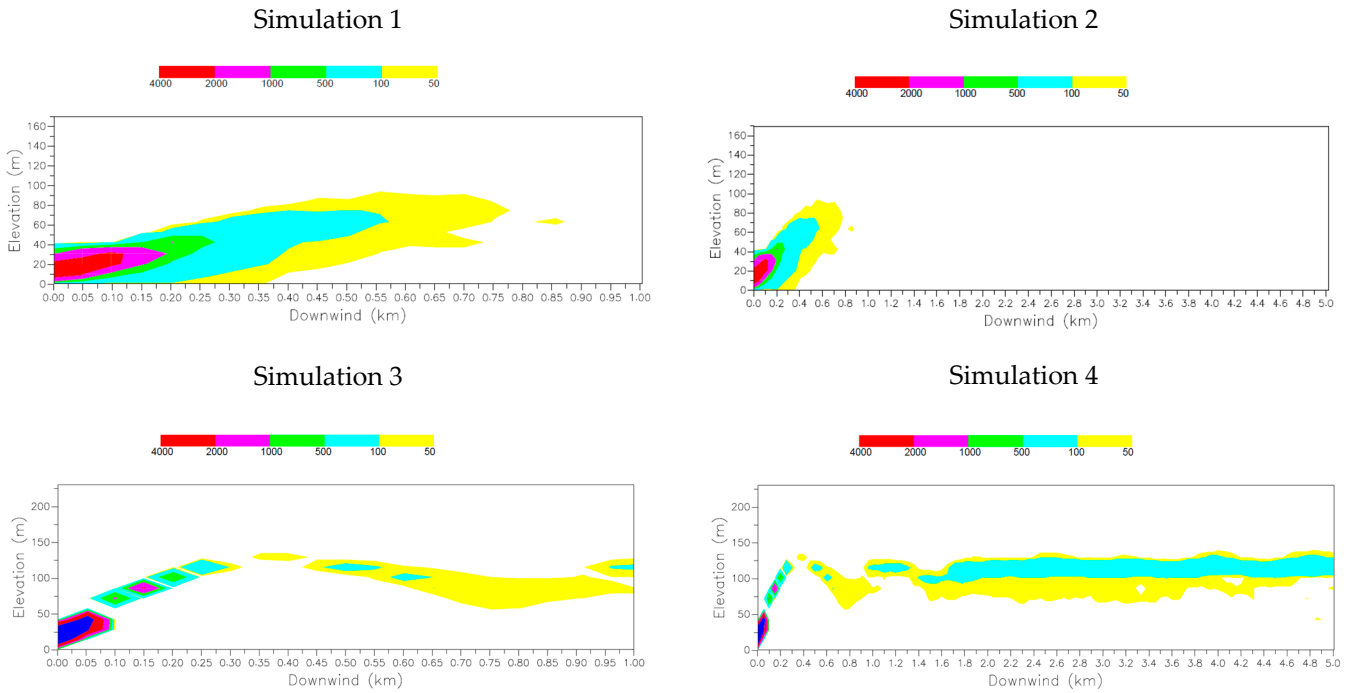


Figure 2. Four graphs showing the variation in the PM10 concentration (micrograms/cubic meter—one-hour average) with respect to downwind distance for four different simulations, labeled 1 through 4. Each simulation represents a different scenario or set of conditions. The x-axis represents the downwind distance, while the y-axis shows the height above ground level of the PM10 concentration. The fire surface area for all four simulations is 50 m^2. These graphs provide visual representations of how PM10 concentrations vary with distance and height under different simulation conditions, which can be useful for understanding the environmental impact and dispersion patterns of particulate matter from fires.

The next four simulations (5 to 8) have a fire surface area of 100 m^2. The first two simulations share a wind velocity of 5 m/s.

In simulation 5, the height of the initial plume is about 40 m (see Figure 3). It is observed that, as the distance increases, the height of the cloud also increases, reaching about 134 m at a distance of 1 km. Initially, there is a concentration of PM10 of more than 4000 μg/m^3, but, after the first 350 m, the latter is reduced to 100–500 μg/m^3. The cloud begins to rise from the ground at a distance of 250 m. At a distance of 802 m downwind, the cloud is 40 m above the ground with concentrations of less than 100 μg/m^3. The plume is not dispersed within 1 km. For simulation 6, unlike simulation 5, the downwind distance is 5 km. The plume, after the first km, is at a height of 67 m above the ground with concentrations between 50 and 100 μg/m^3. The modelled plume after 1.2 km is dispersed with a concentration of less than 50 μg/m^3.

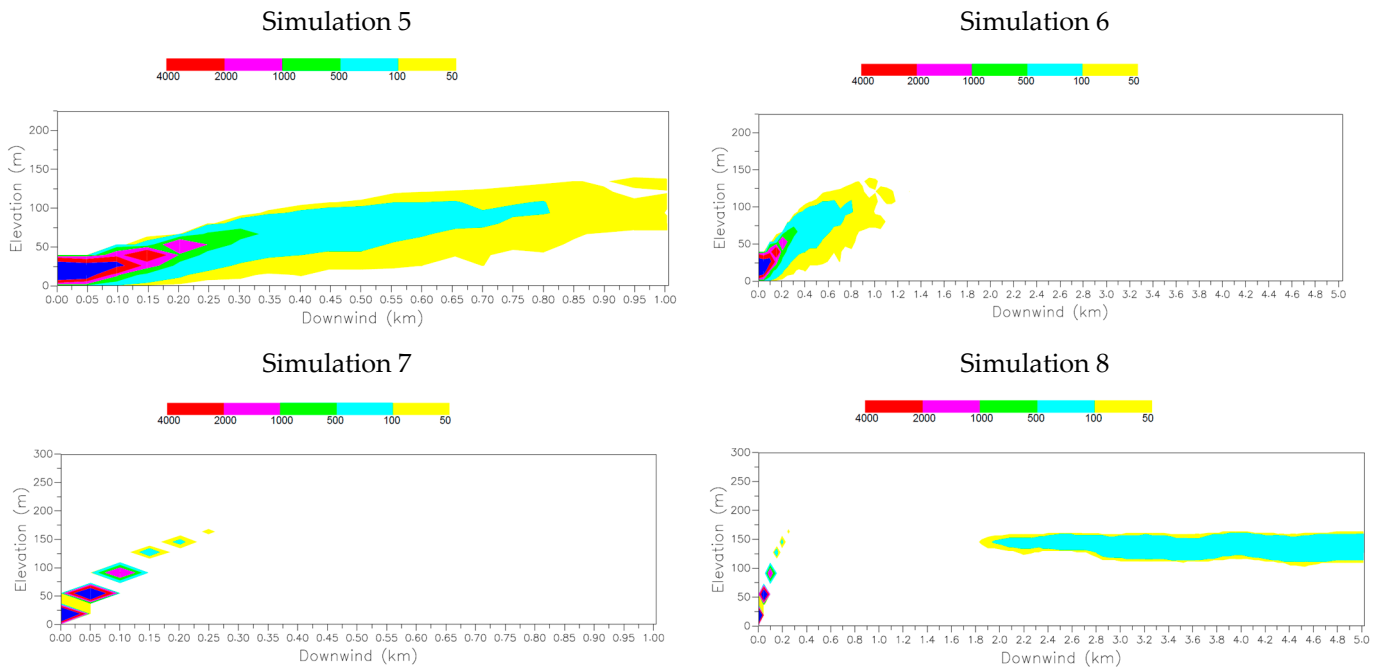


Figure 3. Four graphs showing the variation in the PM10 concentration (micrograms/cubic meter—one-hour average) with respect to downwind distance for four different simulations, labeled 5 through 8. Each simulation represents a different scenario or set of conditions. The x-axis represents the downwind distance, while the y-axis shows the height above ground level of the PM10 concentration. The fire surface area for all four simulations is 100 m^2. These graphs provide visual representations of how PM10 concentrations vary with distance and height under different simulation conditions, which can be useful for understanding the environmental impact and dispersion patterns of particulate matter from fires.

Regarding simulations 7 and 8, they differ from the previous two simulations. The wind speed, this time, is 2 m/s. Reducing the wind speed (simulations 1–2 vs. simulations 3–4) shows how the smoke disperses over greater distances. Moving on to simulation 7, the height of the initial plume is about 54 m (see Figure 3). As the distance increases, the height of the cloud also increases until it reaches almost 163 m at a distance of 250 m. Initially, there is a concentration of PM10 of more than 4000 $\mu g/m^3$; after the first 150 m, it is reduced to 100–500 $\mu g/m^3$. The cloud begins to rise from the ground at a distance of 5 m. At a distance of 250 m downwind, the cloud is 145 m above the ground with concentrations of less than 100 $\mu g/m^3$. It is clear that the plume is not dispersed within 1km. In simulation 8, unlike simulation 7, the downwind distance appears to be 5 km. One can notice that the plume, after the first km, is 109 m above the ground with concentrations between 50 and 500 $\mu g/m^3$.

The last four simulations, 9 to 12, have a fire surface area of 1000 m^2. The first two simulations share a wind velocity of 5m/s.

In simulation 9, the height of the initial plume is about 58 m (see Figure 4). It is observed that, as the distance increases, the height of the cloud also increases until it reaches almost 317 m at a distance of 957 m. At first, there is a concentration of PM10 of more than 4000 $\mu g/m^3$; however, after the first 353 m, it is reduced to 100–500 $\mu g/m^3$. The cloud begins to rise from the ground at a distance of 5 m. The plume is not dispersed within 1 km. When it comes to simulation 10, the downwind distance is 5 km. The plume, after the first km, is 170 m above the ground with concentrations between 50 and 500 $\mu g/m^3$.

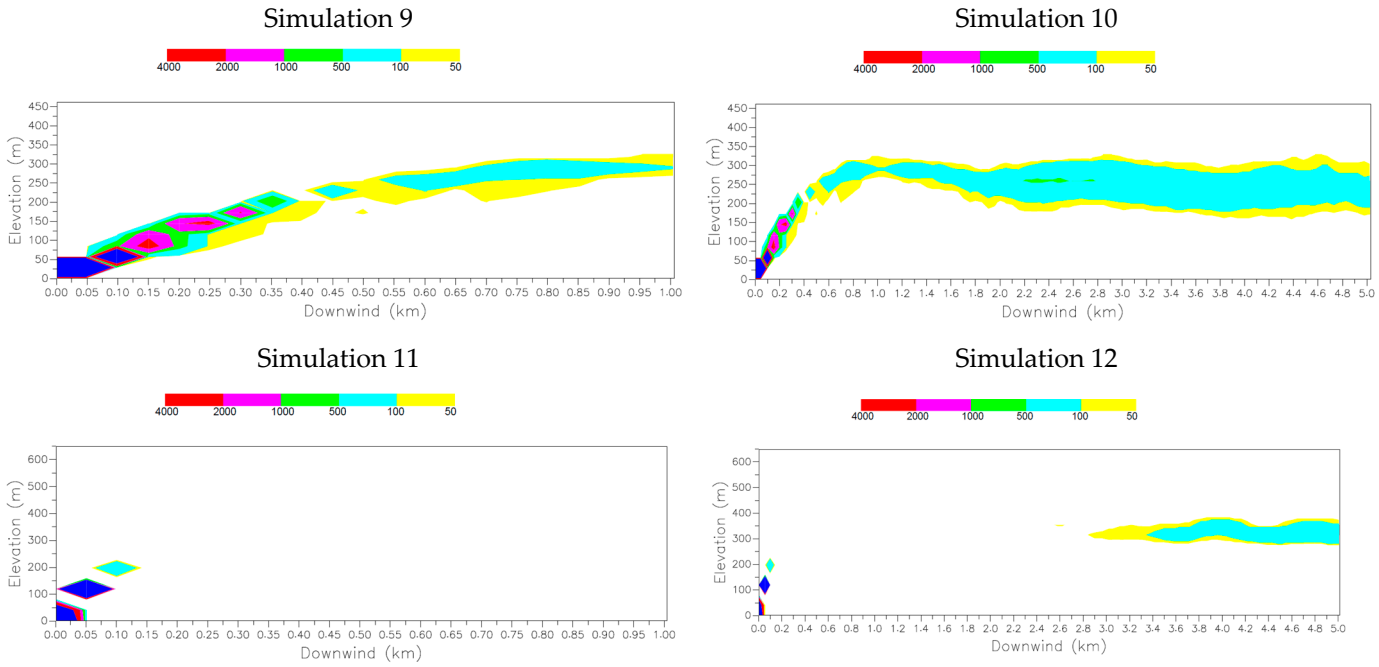


Figure 4. Four graphs showing the variation in the PM10 concentration (micrograms/cubic meter—one-hour average) with respect to downwind distance for four different simulations, labeled 9 through 12. Each simulation represents a different scenario or set of conditions. The x-axis represents the downwind distance, while the y-axis shows the height above ground level of the PM10 concentration. The fire surface area for all four simulations is 1000 m^2. These graphs provide visual representations of how PM10 concentrations vary with distance and height under different simulation conditions, which can be useful for understanding the environmental impact and dispersion patterns of particulate matter from fires.

As we move on to the description of simulations 11 and 12, we can observe how these differ from the previous two simulations. The wind speed, this time, is 2 m/s. Reducing the wind speed (simulations 9–10 vs. simulations 11–12) emphasizes that the smoke disperses over greater distances. For simulation 11, the height of the initial plume is about 78 m (see Figure 4). As the distance increases, the height of the cloud also increases until it is almost 235 m at a distance of 100 m. If, originally, there is a concentration of PM10 of more than 4000 $\mu g/m^3$, after the first 100 m, it is reduced to 100–500 $\mu g/m^3$. The cloud starts to rise from the ground at a distance of 5 m. At a distance of 150 m downwind, the cloud is instead 196 m above the ground with concentrations of less than 100 $\mu g/m^3$. It is clear that the plume is not dispersed within 1 km, so we continue the description with simulation 12, which, unlike simulation 11, has a downwind distance of 5 km. Here, after the first km, the plume is 274 m above the ground with concentrations between 50 and 500 $\mu g/m^3$.

Analyzing the results produced for particulate dispersion, it can be observed that:

- A more stable atmospheric stability class (F) and lower wind velocities affect dispersion, making it more stable and thus able to reach greater distances;
- Finally, an increase in the surface area of the fires increases the production of combustion products; therefore, the quantities of effluents dispersed are greater.

4.2. Emissions of Volatile Organic Compounds (VOCs)

In this section, the 12 simulations (13 to 24) concerning VOC emissions are presented. The conditions are the same as in the previous simulations for PM10. In this case, the results of the simulations are shown in Table 2.

Table 2. Results for simulations 13–24 concerning VOC emissions.

Simulation	Initial Plume Height (m)	Maximum Height (m)	Initial Concentration (μg/m^3)	Maximum Concentration (μg/m^3)	Dispersed Distance with a Concentration of Less than 50 μg/m^3 (m)
13	32	43	100–500	100–500	256
14	32	43	100–500	100–500	256
15	43	101	500–1000	500–1000	201
16	43	101	500–1000	500–1000	201
17	40	67	500–1000	500–1000	303
18	40	67	500–1000	500–1000	303
19	36	109	500–1000	500–1000	150
20	36	109	500–1000	500–1000	150
21	58	202	2000–4000	2000–4000	353
22	58	202	2000–4000	2000–4000	353
23	78	257	2000–4000	2000–4000	100
24	78	257	2000–4000	2000–4000	100

Comparing simulation 13 with simulation 15, it can be concluded that, if all other variables are equal, the process of reducing the wind speed from 5 m/s to 2 m/s results in higher VOCs and higher concentrations. The same applies to simulations 17 and 19 (which have a surface 10 times larger) and for 21 and 23. Observing the results, it can be stated that, in more stable conditions and with lower wind speeds, the presence of VOCs occurs at greater heights than in the case of more turbulent stability classes and higher wind speeds. It could be therefore concluded that, the greater the instability, the greater the presence of VOCs at lower heights above ground.

5. Conclusions

After an overview of the matter at hand, an incidental historical analysis was conducted. The topic, as relevant and contemporary as it is, lends itself to different insights, observations and opinions. It is, however, impossible to ignore how this attention is mainly focused on the aspects related to the storage and disposal of waste rather than on the overall consequences potential fires caused by those substances.

After presenting the variables for modelling the polyethylene fire, simulations were carried out. The modelling of the fire scenario was conducted using the NIST ALOFT tool version 3.10 (NIST SP 924). This software, which can be used on laptops, produces predictions of trajectory and downwind particle concentrations. The interface is user friendly to allow users to input data available from measurements from simple observations. The calculation is thus as accurate as possible for the accident.

The results produced using this software have also been used in the past in real-life situations (deliberate burning case; merchant ship New Carissa, February 1999) [22].

6. Future Developments and Limitations

While the simulations conducted in this study provide valuable insights into the dispersion of toxic effluents from polyethylene fires, there are several limitations that need to be acknowledged and addressed in future research. First, the ALOFT software employed in this study is based on certain simplifying assumptions and approximations, which may not accurately capture the complex dynamics of fire plumes in real-world scenarios. For instance, the model assumes a constant wind speed across the cross-section of the plume,

which may not hold true in turbulent atmospheric conditions. Additionally, the model does not account for the radiative effects of the fire, which can significantly influence the plume behavior, particularly in the near-field region.

Another limitation of the current study is the reliance on literature values for the input parameters, such as the heat release rate, radiative fraction, and burning rate per unit area. These parameters can vary considerably depending on the specific composition and physical properties of the polyethylene waste, as well as the environmental conditions at the fire site. Future studies should aim to obtain more accurate and site-specific input data through experimental measurements or advanced computational fluid dynamics (CFD) simulations.

Furthermore, the simulations presented in this work focused solely on polyethylene as the fuel source. However, in real-world waste storage facilities, the combustible materials can be highly heterogeneous, comprising a mixture of various plastics, paper, textiles, and other organic and inorganic materials. The combustion behavior and effluent composition can vary significantly depending on the fuel composition, necessitating further investigations into the dispersion of toxic effluents from fires involving mixed waste streams.

Despite these limitations, the proposed methodology offers several avenues for future development and refinement. One promising direction is the integration of the ALOFT simulations with other advanced modelling tools, such as CFD simulations or atmospheric dispersion models. By coupling these models, researchers can gain a more comprehensive understanding of the fire dynamics, plume behaviour, and atmospheric transport of pollutants, enabling more accurate predictions and risk assessments.

Another potential area of development is the incorporation of real-time monitoring data into the simulations. By leveraging data from on-site sensors or remote sensing techniques, such as aerial or satellite imagery, the model inputs and boundary conditions can be updated dynamically, allowing for more accurate and responsive simulations during emergency situations.

Moreover, future studies should explore the application of the proposed methodology to different geographical regions and climatic conditions. The atmospheric stability, wind patterns, and topography can significantly influence the dispersion of toxic effluents, necessitating region-specific simulations and validations. Collaboration with local authorities, environmental agencies, and emergency response teams can facilitate the collection of relevant data and the development of tailored strategies for fire prevention and mitigation.

In addition to refining the modelling approach, future research should also focus on the development of mitigation strategies and best practices for waste storage facilities. This could involve the evaluation of fire suppression systems, containment measures, and emergency response protocols, with the aim of minimizing the environmental impact and potential health risks associated with waste fires.

Furthermore, the findings of this study highlight the importance of promoting sustainable waste management practices and reducing reliance on landfills and open-air storage facilities. Efforts should be directed towards enhancing recycling and resource recovery initiatives, as well as exploring alternative waste treatment technologies that minimize the risk of fires and the release of toxic effluents.

Finally, it is crucial to address the socio-economic and regulatory aspects of waste management, particularly in regions where illegal dumping and open burning practices are prevalent. Collaborative efforts involving policymakers, law enforcement agencies, and local communities are essential to combatting these practices and promoting environmentally responsible waste handling and disposal methods.

In conclusion, while the current study provides a valuable foundation for understanding the dispersion of toxic effluents from polyethylene fires, there are numerous

opportunities for future research and development. By addressing the limitations outlined above, incorporating advanced modelling techniques, fostering interdisciplinary collaborations, and promoting sustainable waste management practices, researchers can contribute to the development of more effective fire prevention and mitigation strategies, ultimately safeguarding human health and the environment.

Author Contributions: Conceptualization, G.D.C. and C.V.; methodology, C.V.; software, G.D.C.; validation, G.D.C. and C.V.; formal analysis, G.D.C.; investigation, G.D.C.; resources, C.V.; data curation, G.D.C. and C.V.; writing—original draft preparation, G.D.C. and C.V.; writing—review and editing, G.D.C. and C.V.; visualization, C.V.; supervision, C.V. All authors have read and agreed to the published version of the manuscript.

Funding: This research received no external funding.

Data Availability Statement: Data are contained within the article.

Acknowledgments: The authors wish to thank Giuseppe Maschio and Fabio Dattilo for their attention to this work and valuable suggestions. The authors would also like to thank Vincenzo Puccia for his valuable advice and feedback on the model description.

Conflicts of Interest: The authors declare no conflicts of interest.

References

1. Weiland, S.; Hickmann, T.; Lederer, M.; Marquardt, J.; Schwindenhammer, S. The 2030 agenda for sustainable development: Transformative change through the sustainable development goals? *Politi Gov.* **2021**, *9*, 90–95. [CrossRef]
2. Department of Economic and Social Affairs. Goal 12, Ensure Sustainable Consumption and Production Patterns. Available online: https://sdgs.un.org/goals/goal12 (accessed on 2 February 2025).
3. Reno, J. Waste and Waste Management. *Annu. Rev. Anthr.* **2015**, *44*, 557–572. [CrossRef]
4. Ahmed, R. Innovative Waste Management Solutions: A Global Perspective Challenges and Opportunities and the Bangladesh Context. *Preprints* **2024**. [CrossRef]
5. Demirbas, A. Waste management, waste resource facilities and waste conversion processes. *Energy Convers. Manag.* **2011**, *52*, 1280–1287. [CrossRef]
6. Eurostat Waste Generation and Treatment. Available online: https://ec.europa.eu/ (accessed on 29 October 2022).
7. Ibrahim, M.A.; Göransson, G.; Kaczala, F.; Hogland, W.; Marques, M. Characterization of municipal solid waste temporary storage sites: Risks posed to surrounding areas as a consequence of fire incidents. *Waste Manag.* **2013**, *33*, 2296–2306. [CrossRef]
8. Mikalsen, R.F.; Lönnermark, A.; Glansberg, K.; McNamee, M.; Storesund, K. Fires in waste facilities: Challenges and solutions from a Scandinavian perspective. *Fire Saf. J.* **2021**, *120*, 103023. [CrossRef]
9. Juan, W.Y.; Wu, C.L.; Liu, F.W.; Chen, W.S. Fires in Waste Treatment Facilities: Challenges and Solutions from a Fire Investigation Perspective. *Sustainability* **2023**, *15*, 9756. [CrossRef]
10. Commissione Parlamentare di Inchiesta Sulle Attività Illecite Connesse al Ciclo dei Rifiuti e su Illeciti Ambientali ad Esse Correlati Il Fenomeno degli Incendi Negli Impianti di Trattamento e Smaltimento di Rifiuti. Available online: https://documenti.camera.it/apps/nuovosito/Documenti/DocumentiParlamentari/parser.asp?idLegislatura=17&categoria=023&tipologiaDoc=documento&numero=035&doc=pdfel (accessed on 2 February 2025).
11. McNamee, M.; Meacham, B.; van Hees, P.; Bisby, L.; Chow, W.; Coppalle, A.; Dobashi, R.; Dlugogorski, B.; Fahy, R.; Fleischmann, C.; et al. IAFSS agenda 2030 for a fire safe world. *Fire Saf. J.* **2019**, *110*, 102889. [CrossRef]
12. Battiston, E.; Vianello, C.; Rebuffi, G.; Mocellin, P. Accident Investigation of a Real-Case Fire in a Waste Disposal Facility through Numerical Simulation. *Chem. Eng. Trans.* **2022**, *91*, 565–570. [CrossRef]
13. Romano, G.; Romano, A. Fire Investigation in an Italian Waste Treatment Plant: Lessons Learned and Future Development. In *WIT Transactions on the Built Environment*; WIT Press: Southampton, UK, 2019. [CrossRef]
14. Pizzolante, A.; Nicodemo, F.; Pierri, A.; Ferro, A.; Pierri, B.; Buonerba, C.; Beccaloni, E.; Albanese, S.; Basso, B.; Cerino, P. Development of a municipality index of environmental pressure in Campania, Italy. *Futur. Sci. OA* **2021**, *7*, FSO720. [CrossRef]
15. Falcone, P.M.; De Rosa, S.P. Use of fuzzy cognitive maps to develop policy strategies for the optimization of municipal waste management: A case study of the land of fires (Italy). *Land Use Policy* **2020**, *96*, 104680. [CrossRef]
16. Vasslides, J.M.; Jensen, O.P. Fuzzy cognitive mapping in support of integrated ecosystem assessments: Developing a shared conceptual model among stakeholders. *J. Environ. Manag.* **2016**, *166*, 348–356. [CrossRef] [PubMed]

17. Mazza, A.; Piscitelli, P.; Falco, A.; Santoro, M.L.; Colangelo, M.; Imbriani, G.; Idolo, A.; De Donno, A.; Iannuzzi, L.; Colao, A. Heavy environmental pressure in campania and other italian regions: A short review of available evidence. *Int. J. Environ. Res. Public Health* **2018**, *15*, 105. [CrossRef] [PubMed]
18. Bianchi, F.; Comba, P.; Martuzzi, M.; Palombino, R.; Pizzuti, R. Italian 'Triangle of death'. *Lancet Oncol.* **2004**, *5*, 710. [CrossRef]
19. Mazza, A.; Piscitelli, P.; Neglia, C.; Della Rosa, G.; Iannuzzi, L. Illegal dumping of toxic waste and its effect on human health in Campania, Italy. *Int. J. Environ. Res. Public Health* **2015**, *12*, 6818–6831. [CrossRef]
20. Senior, K.; Mazza, A. Italian 'Triangle of death' linked to waste crisis. *Lancet Oncol.* **2004**, *5*, 525–527. [CrossRef]
21. ISPRA Rapporto Rifiuti Urbani 2022. 2020. Available online: https://www.isprambiente.gov.it/files2020/pubblicazioni/rapporti/rapportorifiutiurbani_ed-2020_n-331-1.pdf (accessed on 31 October 2022).
22. Evans, D.D.; Mulholland, G.W.; Baum, H.R.; Walton, W.D.; McGrattan, K.B. In Situ Burning of Oil Spills. *J. Res. Natl. Inst. Stand. Technol.* **2001**, *106*, 231–278. [CrossRef]
23. Decreto del Presidente Della Repubblica 1 Agosto 2011, n. 151. Available online: https://www.gazzettaufficiale.it/eli/id/2011/09/22/011G0193/sg (accessed on 31 October 2022).
24. Ministero Dell'interno Decreto 3 Agosto 2015. 2015. Available online: https://www.gazzettaufficiale.it/eli/id/2015/08/20/15A06189/sg (accessed on 31 October 2022).
25. Verma, R.; Vinoda, K.S.; Papireddy, M.; Gowda, A.N.S. Toxic Pollutants from Plastic Waste—A Review. *Procedia Environ. Sci.* **2016**, *35*, 701–708. [CrossRef]
26. Hodgkin, J.H.; Galbraith, M.N.; Chong, Y.K. Combustion Products from Burning Polyethylene. *J. Macromol. Sci. Chem.* **1982**, *17*, 35–44. [CrossRef]
27. Guillaume, E.; Marlair, G.; Delacroix, A.; Drysdale, D. Considerations on combustion and fire behaviour of materials: A change of mind during the 18th century. *J. Fire Sci.* **2015**, *34*, 69–84. [CrossRef]
28. Dhakal, H.N.; Ismail, S.O. Introduction to Composite Materials. In *Sustainable Composites for Lightweight Applications*; Elsevier: Amsterdam, The Netherlands, 2021; pp. 1–16. [CrossRef]
29. Kumar, N.; Ukey, P.D.; Francis, V.; Singh, R.P.; Sahu, S. Plastic Pellets. In *Polymers for 3D Printing: Methods, Properties, and Characteristics*; Elsevier: Amsterdam, The Netherlands, 2022; pp. 307–323. [CrossRef]
30. Morris, B.A. Designing Flexible Packaging for Sustainability. In *The Science and Technology of Flexible Packaging*; Elsevier: Amsterdam, The Netherlands, 2022; pp. 709–761. [CrossRef]
31. Hull, D.; Clyne, T.W. *An Introduction to Composite Materials*; Cambridge University Press (CUP): Cambridge, UK, 1996. [CrossRef]
32. Silvestre, J.; Silvestre, N.; De Brito, J. An overview on the improvement of mechanical properties of ceramics nanocomposites. *J. Nanomater.* **2015**, *2015*, 106494. [CrossRef]
33. Plastic Packaging Waste: 38% Recycled in 2020—Products Eurostat News—Eurostat. Available online: https://ec.europa.eu/eurostat/web/products-eurostat-news/-/ddn-20221020-1 (accessed on 2 February 2025).
34. Janajreh, I.; Adeyemi, I.; Elagroudy, S. Gasification feasibility of polyethylene, polypropylene, polystyrene waste and their mixture: Experimental studies and modeling. *Sustain. Energy Technol. Assess.* **2020**, *39*, 100684. [CrossRef]
35. Piao, M.; Chu, S.; Zheng, M.; Xu, X. Characterization of the combustion products of polyethylene. *Chemosphere* **1999**, *39*, 1497–1512. [CrossRef]
36. Ghoniem, A.F.; Zhanga, X.; Knioa, O.; Baum, H.R.; Rehm, R.G. Dispersion and deposition of smoke plumes generated in massive fires. *J. Hazard. Mater.* **1993**, *33*, 275–293. [CrossRef]
37. Walton, W.D.; McGrattan, K.B.; Mullin, J.V. ALOFT-PC: A Smoke Plume Trajectory Model for Personal Computers. 2003. Available online: https://www.nist.gov/publications/aloft-pc-smoke-plume-trajectory-model-personal-computers (accessed on 30 October 2022).
38. Walton, W.; McGrattan, K. *Smoke Plume Trajectory from In Situ Burning of Crude Oil in Alaska—Updated Simulation Results*; NIST Technical Note; U.S. Department of Commerce, National Institute of Standards and Technology: Gaithersburg, MD, USA, 2011.
39. McGrattan, K.B.; Baum, H.R.; Walton, W.D.; Trelles, J.J. *Smoke Plume Trajectory From In Situ Burning of Crude Oil in Alaska: Field Experiments and Modeling of Complex Terrain (NISTIR 5958)*; U.S. Department of Commerce, National Institute of Standards and Technology: Gaithersburg, MD, USA, 1997. [CrossRef]
40. Josephson, A.J.; Castaño, D.; Koo, E.; Linn, R.R. Zonal-Based Emission Source Term Model for Predicting Particulate Emission Factors in Wildfire Simulations. *Fire Technol.* **2020**, *57*, 943–971. [CrossRef]
41. Josephson, A.J.; Castaño, D.; Holmes, M.J.; Linn, R.R. Simulation comparisons of particulate emissions from fires under marginal and critical conditions. *Atmosphere* **2019**, *10*, 704. [CrossRef]
42. Zengel, S.A.; Michel, J.; Dahlin, J.A. Environmental effects of in situ burning of oil spills in inland and upland habitats. *Spill Sci. Technol. Bull.* **2003**, *8*, 373–377. [CrossRef]
43. Trelles, J.; McGrattan, K.B.; Baum, H.R. Smoke Dispersion from Multiple Fire Plumes. *AIAA J.* **2012**, *37*, 1588–1601. [CrossRef]
44. Kahl, J.D.W.; Chapman, H.L. Atmospheric stability characterization using the Pasquill method: A critical evaluation. *Atmospheric Environ.* **2018**, *187*, 196–209. [CrossRef]

45. Slade, D.H. Meteorology and Atomic Energy. Environmental Science Services Administration: Silver Spring, MD, USA, 1968. [CrossRef]
46. Lees, F.P. *Lees' Loss Prevention in the Process Industries*, 4th ed.; Butterworth-Heinemann: Oxford, UK, 2012. [CrossRef]
47. S., O.G. Atmospheric diffusion. By F. Pasquill. London (Van Nostrand Co.), 1962. Pp. xii, 297; 60s. *Q. J. R. Meteorol. Soc.* **1962**, *88*, 202–203. [CrossRef]
48. Scire, J.S.; Strimaitis, D.G.; Yamartino, R.J. *A User's Guide for the CALPUFF Dispersion Model*; UBC Earth, Ocean and Atmospheric Sciences: Vancouver, BC, USA, 2000.
49. Offshore and Coastal Dispersion (OCD) Model. Users Guide. Available online: https://inis.iaea.org/records/a5sq7-8fx37 (accessed on 2 February 2025).
50. Lyon, R.E.; Janssens, M.L. Polymer Flammability. *Am. Chem. Soc. Polym. Prepr. Div. Polym. Chem.* **1985**, *26*, 1–70. [CrossRef]
51. Wu, D.; Li, Q.; Shang, X.; Liang, Y.; Ding, X.; Sun, H.; Li, S.; Wang, S.; Chen, Y.; Chen, J. Commodity plastic burning as a source of inhaled toxic aerosols. *J. Hazard. Mater.* **2021**, *416*, 125820. [CrossRef] [PubMed]
52. Aurell, J.; Gullett, B.K.; Yamamoto, D. Emissions from open burning of simulated military waste from forward operating bases. *Environ. Sci. Technol.* **2012**, *46*, 11004–11012. [CrossRef] [PubMed]
53. Philip, J. *SFPE Handbook of Fire Protection Engineering*, 3rd ed.; Editorial Staff the Following are Registered Trademarks of the National Fire Protection Association: National Electrical Code® and NEC® National Fire Codes® Life Safety Code® and 101 ® National Fire Alarm Code® and NFPA 72® NFPA and Design Logo; National Fire Protection Association: Quincy, MA, USA, 2002.
54. Review of Emission Factors for Incident Fires Innovation for Efficiency Science Programme Science Report: SC060037/SR3. Available online: https://assets.publishing.service.gov.uk/media/5a7c7177e5274a5255bceadc/scho0809bqut-e-e.pdf (accessed on 2 February 2025).
55. De Cet, G. Analisi di Effluenti Tossici Prodotti da Incendio di Stoccaggi di Rifiuti. University of Padua, 2018. Available online: https://thesis.unipd.it/handle/20.500.12608/28265 (accessed on 30 October 2022).
56. Hurley, M.J.; Gottuk, D.T.; Hall Jr, J.R.; Harada, K.; Kuligowski, E.D.; Puchovsky, M.; Watts, J.M.; Wieczorekc, J. *SFPE Handbook of Fire Protection Engineering*, 5th ed.; Springer Nature: Dordrecht, The Netherlands, 2016. [CrossRef]
57. Shemwell, B.E.; Levendis, Y.A. Particulates generated from combustion of polymers (plastics). *J. Air Waste Manag. Assoc.* **2000**, *50*, 94–102. [CrossRef]
58. Hilado, C.J. *Plastics Flammability Handbook*; Carl Hanser Verlag: Muenchen, Germany, 2004. [CrossRef]
59. Lyon, R.E.; Janssens, M.L. Flammability. In *Encyclopedia of Polymer Science and Technology*; Springer: New York, NY, USA, 2005. [CrossRef]

Disclaimer/Publisher's Note: The statements, opinions and data contained in all publications are solely those of the individual author(s) and contributor(s) and not of MDPI and/or the editor(s). MDPI and/or the editor(s) disclaim responsibility for any injury to people or property resulting from any ideas, methods, instructions or products referred to in the content.